

Direct measurement of muonium hyperfine frequencies in Si and Ge

Eugen Holzschuh

Physik-Institut, Universität Zürich, 8001 Zürich, Switzerland

(Received 28 June 1982)

The hyperfine frequency ν_0 of normal muonium Mu has been measured as a function of temperature in zero magnetic field with an apparatus of high time resolution. Compared with the usual two-frequency method, the direct measurement of ν_0 typically gives more accurate results by a factor of 10. For Mu in Ge, ν_0 shows a monotonic decrease with increasing temperature which is well described by a Debye model. For Mu in Si, ν_0 exhibits a nonmonotonic temperature variation with a maximum at 80 K. By a measurement with external pressure up to 1.5 kbar it is shown that the nonmonotonic lattice expansion of Si cannot cause the observed effect. Rapid relaxation of the direct transition was observed in Si below 20 K. A similar anomaly of the triplet transition signals in a magnetic field could not be found. A model is presented which assumes diffusion of Mu over slightly different sites and which explains all observed effects consistently.

I. INTRODUCTION

Two methods have been traditionally used for studying the formation and the behavior of muonium (μ^+e^-) in solids. With the longitudinal-field technique, Feher *et al.*^{1,2} and Andrianow *et al.*³ could demonstrate the formation of muonium in Si and Ge at low temperature. This method, however, is rather insensitive and allows only rough estimates of the hyperfine interaction (HFI) between the muon and its bound electron.

A considerable improvement is possible with the two-frequency method, introduced by Gurevich *et al.*⁴ It could be shown that the so-called normal muonium Mu in Si and Ge is well described by a spin Hamiltonian with the same form as for muonium or hydrogen in vacuum,

$$H = h\nu_0 \vec{I} \cdot \vec{S} - g_e \mu_B^e \vec{S} \cdot \vec{B} - g_\mu \mu_B^\mu \vec{I} \cdot \vec{B}, \quad (1)$$

but with a hyperfine frequency ν_0 reduced by approximately a factor of 2. \vec{I} and \vec{S} are the spin operators of the muon and the electron, respectively, and \vec{B} denotes the applied magnetic field. The strength of the hyperfine interaction is proportional to the electron density at the muon site; we write

$$h\nu_0 = -\frac{8\pi}{3} g_e g_\mu \mu_B^\mu \mu_B^e |\psi(0)|^2. \quad (2)$$

Measured values are⁵ $\nu_0(\text{Si}) = 0.44\nu_0(\text{vac})$ and⁶ $\nu_0(\text{Ge}) = 0.53\nu_0(\text{vac})$ with the vacuum value⁷ $\nu_0(\text{vac}) = 4463.302 \text{ MHz}$. The energy eigenvalues

of Eq. (1) are plotted in Fig. 1 for Mu in Si. The transition frequencies ν_{12} and ν_{23} are observed with the two-frequency method. Only the difference $\nu_{23} - \nu_{12}$ determines ν_0 , whereas the sum $\nu_{23} + \nu_{12}$ is mainly a measure of the applied field.

Conceptually simpler than the two-frequency method and, as will be shown, still more accurate is the direct method, i.e., the measurement of the triplet-singlet transition in zero applied field (see Fig. 1). For this case the time-dependent muon polarization calculated from Eq. (1) with $B=0$ is given by

$$\vec{P}_\mu(t) = \frac{1}{2} [1 + \cos(2\pi\nu_0 t)] \vec{P}_\mu(0), \quad (3)$$

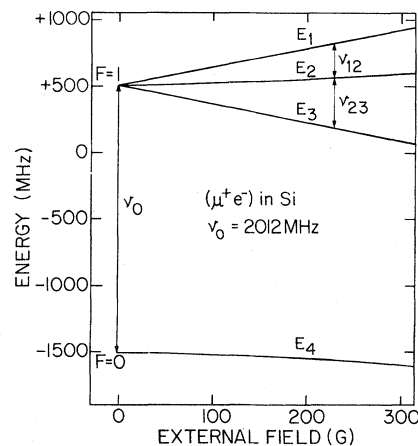


FIG. 1. Breit-Rabi diagram of normal muonium in Si. Transitions observed by the direct method (ν_0) and by the two-frequency method (ν_{12} and ν_{23}) are indicated.

where $t=0$ refers to the time of muonium formation. Thus in a muon-spin-rotation (μ SR) experiment⁸ a signal should be observed with frequency ν_0 , provided the measurement can be done with a sufficient time resolution. For Mu in Si and Ge with ν_0 of the order of 2 GHz, this is easily achieved. As it turned out, the direct method is even applicable for muonium in quartz with $\nu_0=4.5$ GHz.⁹

A discussion of the effects of finite time resolution on high-frequency signals is given in Sec. II A, and a description of the apparatus follows in Sec. II B. Using plastic scintillator detectors, a time resolution of 150–250 ps full width at half maximum (FWHM) was achieved, as compared with usual μ SR apparatus with typically 1.0–1.5 ns FWHM. This improvement was possible mainly because without an external field no long light guides between scintillators and photomultiplier tubes are necessary.

The main purpose of the present investigation was the measurement of the temperature dependence of ν_0 for Mu in Si and Ge by the direct method (see Secs. III A and III B). Such effects have been searched for earlier,^{10,11} but because of the limited precision of the two-frequency method they were not found.

A variation of ν_0 with temperature may result from lattice expansion or from dynamic effects. By a measurement with high pressure (see Sec. III C) it could be shown that the former mechanism gives a negligible contribution to the observed effects for Mu in Si.

Lattice vibrations produce dynamic distortions of the local Mu environment. As has been shown by Šimánek and Orbach¹² for Mg^{2+} in MgO, in the long-wavelength limit this leads to a temperature variation of the hyperfine interaction proportional to the mean-square strain $\langle \epsilon^2 \rangle$. Assuming a Debye spectrum for the acoustic phonons and neglecting the optical phonons, $\langle \epsilon^2 \rangle$ is proportional to the total heat. Our data for Mu in Ge can be fitted to this Debye model. The hyperfine frequency of Mu in Si, however, shows a nonmonotonic temperature dependence, indicating that an additional process is effective.

Recently, a temperature-dependent HFI for anomalous muonium Mu^* in Si (Ref. 13) and in diamond¹⁴ was reported. Mu^* is another paramagnetic state formed by positive muons in diamond, Si (Refs. 5 and 15) and Ge.⁶ The data for Mu^* could also be well described by the Debye model. In Sec. IV we compare them with the results for Mu.

Extensive studies of the spin relaxation of Mu in Si (Refs. 16–18) and Ge (Ref. 19) have been performed, showing a rich variety of temperature- and doping-dependent effects. In these studies only the transitions ν_{12} and ν_{23} (see Fig. 1) were observed. A comparison with the quite different transition ν_0 may thus shed light on the underlying processes. Indeed we find that there are large differences at low temperature. This allows us to argue in connection with the temperature dependence of ν_0 , that Mu is mobile in the temperature range investigated.

II. EXPERIMENTAL DETAILS

In a μ SR experiment, positive spin-polarized muons are stopped in the sample to be investigated, and the positrons from the anisotropic muon decay ($\tau_\mu=2.2$ μ s) are recorded as a function of the time after a muon stop. Since positron emission is most probable in the direction of the muon spin, the exponential muon decay is modulated with the precession or oscillation frequencies of the muon spin. If muonium is formed, these frequencies correspond to transitions between the energy levels of the Hamiltonian equation (1).

A. Timing

For large frequencies, the effects of the finite time resolution of the particle detectors must be considered. In general, the modulation spectrum consists of a sum of terms like

$$f(t) = ae^{-\lambda t} \cos(\omega t), \quad t > 0 \quad (4)$$

where an exponential damping is assumed. Let $g(t)$ be the normalized time-resolution function of the detectors. The observed signal is then the convolution of g with f ,

$$f_{\text{obs}}(t) = \int g(t-t')f(t')dt' \quad (5)$$

In realistic cases, g is a “peaked” function, which is appreciably different from zero over only a small time interval. For t much larger than the width of g , Eq. (5) may be written as

$$\begin{aligned} f_{\text{obs}}(t) &\simeq a \operatorname{Re} \exp(i\omega t - \lambda t) \\ &\times \int g(t') \exp(-i\omega t' + \lambda t') dt' \\ &= ae^{-\lambda t} \operatorname{Re} c e^{i\omega t} \end{aligned} \quad (6)$$

The constant c ($|c| < 1$) describes the reduction of the measured signal amplitude and, if g is not an even function, a phase shift. It is important to note,

however, that the form and in particular the frequency of the measured signal are independent of the shape of g . To evaluate Eq. (6), a Gaussian g with $\Delta t = \text{FWHM}$ may be assumed. Then c is real and with $\nu = \omega/2\pi$ and $\lambda \equiv 0$ given by

$$c = \frac{a_{\text{obs}}}{a} = \exp \left[\frac{-(\pi\nu\Delta t)^2}{4 \ln 2} \right]. \quad (7)$$

Accordingly, Δt should be less than about $1/(2\nu)$ to obtain a reasonable signal. For Mu in Si and Ge, this means $\Delta t \lesssim 250$ ps.

B. Detector arrangement

The zero-field experiments were done with an apparatus similar to other μSR setups, but special care was taken to achieve a high time resolution of the detectors and to maintain a compact geometry around the target. A schematic view of the detector arrangement is shown in Fig. 2.

The muon beam is collimated by three lead collimators to a final diameter of 12 mm, degraded by CH_2 , and stopped in the target inside a He flow cryostat. The plastic scintillators B_1 , B_2 , M , and E give logic signals necessary to distinguish the various possible events such as incoming muons, stopped muons and decay positrons.

The timing detectors M_t and E_t consist of 10-mm-thick NE 111 plastic scintillators attached to XP2020 photomultiplier tubes. The M_t scintillator has a $20 \times 20\text{-mm}^2$ cross section and a 15-mm long light guide. For E_t , scintillator disks with 20-, 30-, and 50-mm diameter were used. In the latter case a short conical light guide, not shown in Fig. 2, was inserted. The XP2020 tubes are selected units from a sample of ten.

The anode pulses from the timing detectors are

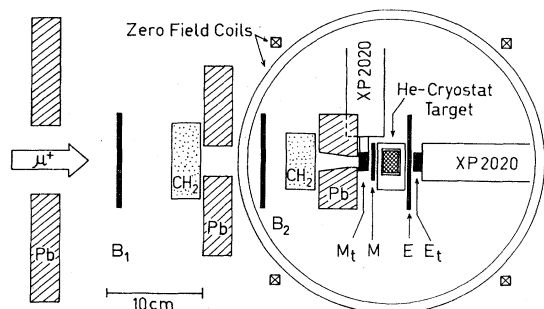


FIG. 2. Schematic view of the detector arrangement. Shown are the scintillators (black), the lead collimators (Pb), the degrader (CH_2), the cryostat with the target inside, and the photomultipliers (XP2020) of the timing detectors.

discriminated by Ortec 583 differential constant fraction discriminators and, if coincident with the appropriate logic signals, are fed into the start (M_t) and the stop (E_t) input of a time-to-amplitude converter (TAC). The TAC time information is digitized by a 13-bit analog-to-digital converter (ADC) and then a histogram with 8192 channels is formed in the memory of an on-line computer.

In the experiment, the 583-discriminators were adjusted with a ^{60}Co source, i.e., without beam. The time resolution Δt turned out to depend strongly on the diameter of the E_t scintillator. Values of 150, 210, and 250 ps FWHM were achieved in actual μSR experiments with diameters of 20, 30, and 50 mm, respectively. These Δt values were obtained with Eq. (7) by measuring the ratio of the amplitudes of signals with frequency ν_0 in zero field and $\nu_{12} \approx \nu_{23} \ll \nu_0$ in a small field and comparing with the theoretical amplitude ratio for $\Delta t = 0$. The width of the prompt muon peak, i.e., from muons which pass all counters, was always appreciably smaller than Δt . This is because muons produce more light in the scintillator E_t as compared with positrons and because the collimated beam hits E_t mainly in the center.

C. High-pressure cell

The cell used for the measurement with hydrostatic pressure (Sec. III C) is shown in Fig. 3. The sample container is a tube, fabricated from a titanium alloy with 6 wt. % Al and 4 wt. % V (Luftfahrt-W.Nr. 37164). The specified tensile strength for a permanent deformation of 0.2% is 825 N/mm^2 . The tube has an inner diameter of 20 mm and a wall thickness of 2.4 mm. The cell is sealed with a stainless-steel cap screwed on the Ti tube, a Cu disk, and a 6-mm-thick stainless-steel disk. The Cu disk is pressed on the sharp edge of the Ti tube by six screws arranged circularly in the cap. The cell with the sample inside and the inlet pipe were filled with oil.

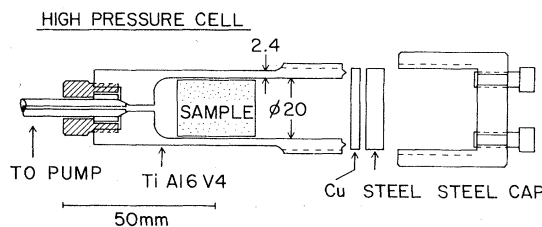


FIG. 3. Design of the pressure cell. Dimensions in mm.

The pressure was produced by an oil handpump and measured with a manometer with ± 30 bar accuracy. Pressure loads up to 1500 bar were applied repeatedly. The permanent deformations remained smaller than a few 1/100 mm for the Ti-tube diameter.

III. MEASUREMENTS AND RESULTS

Normal muonium Mu in Ge and Si was investigated by the direct method in the temperature range in which Mu signals are also observed with the two-frequency method, i.e., up to 90 K for Ge and up to 290 K for Si. The samples used were single crystals of the highest commercially available purity. The specified concentration of electrically active impurities was $\sim 10^{10} \text{ cm}^{-3}$ for the Ge crystal (General Electric) and $\sim 5 \times 10^{11} \text{ cm}^{-3}$ (*p*-type) for the Si crystal (Hoboken). For the pressure experiment (Sec. III C), a different Si crystal (Wacker), also *p* type with $\sim 10^{12} \text{ cm}^{-3}$ electrically active impurities, was used.

The experiments were performed at the Swiss Institute for Nuclear Research (SIN), where intense beams of spin-polarized muons from the superconducting muon channels are available. In each run, the time-dependent data were accumulated in a histogram with 7500 usable channels 45-ps wide, giving time spectra 350-ns long. The rate of accumulated events was 400–600 s^{-1} at a muon stop rate of 35000 s^{-1} . A total of $(5-10) \times 10^6$ good events were taken for each run.

The earth's field was compensated by three pairs of "zero-field" coils (see Fig. 2) to a value smaller than 0.05 G. The residual field theoretically leads to a splitting of the singlet-triplet transition (see Fig. 1), however in such a way that, independent of the direction of the field, the center of gravity of the lines is not shifted. Thus, no systematic error for ν_0 is possible, and within the length of the time spectra taken, only a small additional damping of about $0.3 \mu\text{s}^{-1}$ may be expected.

The data were analyzed by least-squares fits assuming an exponential signal damping of the form $R(t) = \exp(-\lambda t)$. The global nonlinearity of the time scale of about 10^{-3} produced by the time-measuring devices TAC and ADC were taken into account.

A. Mu in Ge, temperature dependence

Part of a Fourier-transformed spectrum obtained from a run with Ge at 15 K is shown in Fig. 4. The

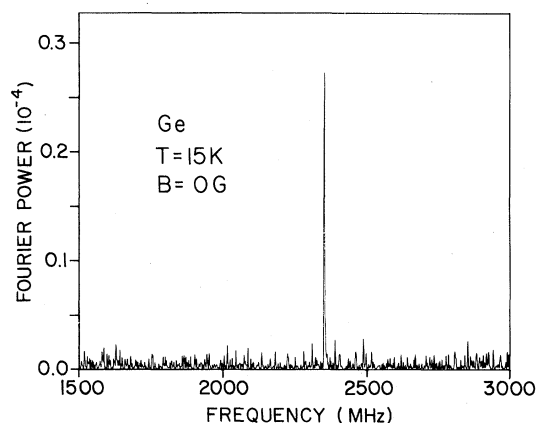


FIG. 4. Part of a Fourier-transformed spectrum showing the line of the direct transition of Mu in Ge at $\nu_0 \approx 2360$ MHz.

line at 2360 MHz corresponds to the expected triplet-singlet transition in zero field with frequency ν_0 (see Fig. 1). In Fig. 5 the measured values of ν_0 are plotted as a function of temperature. The overall variation is about 1%. The data are well described by the formula¹²

$$\nu_0(T) = \nu_0(0) \left[1 - C \left(\frac{T}{\Theta} \right)^4 \int_0^{\Theta/T} \frac{x^3 dx}{e^x - 1} \right], \quad (8)$$

which may be derived under the assumption that Mu couples to the long-wavelength part of a Debye spectrum of acoustic phonons. A least-squares fit of Eq. (8) to the Ge data gives the following parameter values:

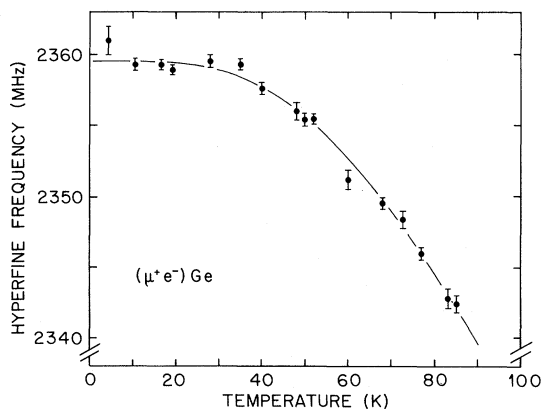


FIG. 5. Measured hyperfine frequencies ν_0 of Mu in Ge as a function of temperature. The curve is calculated with Eq. (8) (Debye model) and with the fitted parameters given in Eq. (9).

$$\begin{aligned} \nu_0(0) &= 2359.5 \pm 0.2 \text{ MHz}, \\ C &= 0.27 \pm 0.07, \\ \Theta &= 273 \pm 25 \text{ K}. \end{aligned} \quad (9)$$

The curve in Fig. 5 was calculated from Eq. (8) with these parameters.

The value of $\nu_0(0)$ compares well with recent results obtained by the two-frequency method. Balzer *et al.*¹¹ obtained 2359 ± 2 MHz as a weighted average from many temperature dependent measurements. Since their data show rapidly increasing errors above 40 K because of increasing signal damping, this is actually a low-temperature value. Within errors the two methods thus give the same results for ν_0 .

The fitted value of Θ appears somewhat small when compared with the averaged Debye temperature $\bar{\Theta}_D = 360$ K of Ge given in the literature.²⁰ It must be kept in mind, however, that the calorimetric Debye Θ_D of Ge depends strongly on temperature,²¹ varying between 250 and 370 K in the interval of our measurements.

As has been shown by Calvo and Orbach,²² the coupling constant C is a measure of the effect of the zero-point motion of the lattice. Within the Debye model, the following relation holds:

$$\nu_0(\text{RL}) = \nu_0(0)(1 + C/8), \quad (10)$$

where $\nu_0(\text{RL})$ is the hyperfine frequency for Mu in a rigid lattice. This may be important when interpreting the results of theoretical calculations, which usually do not take into account the zero-point motion. In Sec. IV we compare C with other muon results.

An alternative to the Debye model is to assume that only one phonon mode with frequency ν_p is causing the temperature dependence of ν_0 . This would be a reasonable approximation if only optical phonons were important. ν_0 should then vary as²³

$$\nu_0(T) = \nu_0(0) \{ 1 - \tilde{C} [\exp(\tilde{\Theta}/T) - 1] \}, \quad (11)$$

where $\tilde{\Theta} = h\nu_p/k_B$. The data of Fig. 5 can equally well be fitted to this formula, giving $\nu_p = (3.6 \pm 0.3) \times 10^{12}$ Hz. This frequency, however, cannot be associated with any particular feature in the phonon distribution²¹ of Ge and is more than a factor of 2 smaller than the frequencies of the optical phonons, which are in the range $(8-9) \times 10^{12}$ Hz. We will therefore not consider Eq. (11) further.

B. Mu in Si, temperature dependence

The measured hyperfine frequencies for Mu in Si are plotted in Fig. 6 as a function of temperature.

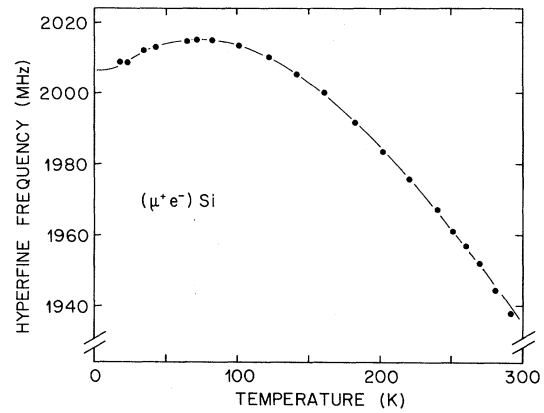


FIG. 6. Measured hyperfine frequencies ν_0 of Mu in Si as a function of temperature. The errors are typically 2 to 4 times smaller than the size of the data points. The curve is calculated with Eq. (14) and with the fitted parameters given in Eq. (15).

The errors are typically a factor of 2–4 smaller than the size of the data points. The overall variation is about 4%. Because of the maximum at 80 K, the simple formula given by Eqs. (8) and (11) cannot describe the data.

One may attribute this anomaly to the nonmonotonic thermal lattice expansion of Si which produces a minimum of the lattice constant a at 120 K.²⁴ We have tried to fit the Si data under the assumption that the prefactor $\nu_0(0)$ appearing in Eq. (8) is a function of the change $\delta a(T)$ of the lattice constant,²⁵ which may be linearized for small $\delta a(T)$, thereupon introducing a fourth parameter $\partial\nu_0/\partial a$. This still gave a very bad fit and a unphysically large value $\partial\nu_0/\partial a \simeq 70\,000$ MHz/Å. The result of the pressure experiment (Sec. III C), which may be anticipated here, confirmed that lattice expansion causes negligible effects on ν_0 .

There are other anomalies observed for Mu in Si at low temperature which appear important in the present context and which we summarize in the following.

(a) The signal of the direct transition abruptly disappeared below 18 K: Spectra taken at 10 and 12 K did not show a signal. The relaxation rate λ_0 of the direct transition is plotted in Fig. 7. Whereas the rise of λ_0 at high temperatures is similar to the behavior of the relaxation rate λ_t of the intratriplet transitions, the rise of λ_0 below 20 K is apparently not observed for λ_t .¹⁶

(b) We have investigated λ_t more carefully in the range 4.5–50 K and for fields up to 220 G using our standard μSR apparatus²⁶ and the same Si crystal as for the measurements of ν_0 . No noteworthy

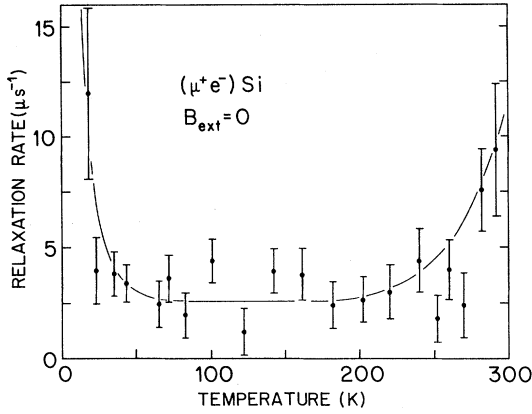


FIG. 7. Relaxation rate λ_0 of the direct transition of Mu in Si. The curve is only a guide to the eye.

anomaly was observed. The measured amplitudes and relaxation rates λ_t for 10 G are plotted in Fig. 8. For this case the two frequencies ν_{12} , ν_{23} are almost equal and were not resolved. Within a statistical error of $\pm 0.5 \mu\text{s}^{-1}$, also no field dependence of λ_t was detected.

(c) Bucci *et al.*¹⁷ measured λ_t of Mu in Si down to 60 mK at $B=6$ G. For $T \lesssim 0.5$ K $\lambda_t = 4 \mu\text{s}^{-1}$ was constant, then decreased in the range 0.5–5 K to $2 \mu\text{s}^{-1}$, and again stayed constant at this value up to 50 K. These authors also looked for an anisotropic part of the hyperfine interaction and claimed that it is smaller than 0.05% of the isotropic part.

The constant amplitude in Fig. 8 shows that Mu is formed with a temperature-independent probability. This together with case (a) implies that λ_0 is larger than $20 \mu\text{s}^{-1}$ at 10 K.

Muonium depolarization is usually interpreted^{27,19} in terms of random magnetic fields, chemical

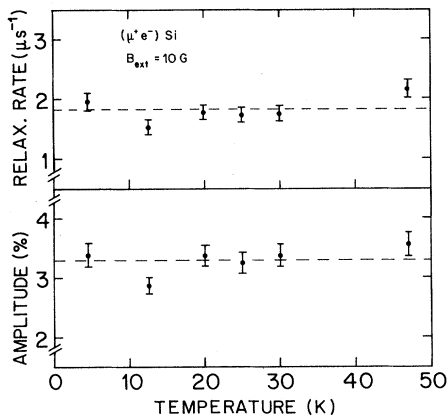


FIG. 8. Relaxation rate λ_t and amplitude of the triplet signal of Mu in Si in 10-G applied field.

reactions of Mu, or spin flips of the bound electron by conduction electrons or Raman effects. These processes, however, give within a factor of about 2 the same values for λ_t and λ_0 . All observations may be explained consistently if it is assumed that Mu is diffusing among at least two different sites.

In regard to cases (a) and (b) a difference $\delta\nu_0$ of the hyperfine frequency for Mu at different sites causes [Eq. (1)] a difference for the intratriplet frequencies to first order given by

$$\delta\nu_{12} = -\delta\nu_{23} = \frac{x^2}{4} \delta\nu_0, \quad (12)$$

where

$$x = 2.82B/\nu_0, \quad (13)$$

for B in G and ν_0 in MHz is small even at $B=200$ G. Thus slow hopping may cause large damping for the transition ν_0 and negligible effects on the transitions ν_{12} and ν_{23} . Concerning case (c), apparently Mu in Si becomes mobile at 1 K and averages small magnetic perturbations such as interactions with the nuclear dipolar moments of the ^{29}Si isotopes.

The temperature dependence of ν_0 (Fig. 6) may now be explained as follows: To observe the transition ν_0 , the mean hopping time τ_c must satisfy $\tau_c \leq 10 \mu\text{s}^{-1}/(\pi\delta\nu_0)^2$. The measured frequency is then an average where each site is occupied according to a Boltzmann factor. For simplicity we assume two sites with equal abundance. We assume further that the phonon-induced shift of ν_0 is the same for both sites and given by Eq. (8). Putting things together one obtains

$$\nu_0(T) = \left[\nu_0(0) + \frac{\delta\nu_0}{e^{\Theta'/T} + 1} \right] \times \left[1 - C \left(\frac{T}{\Theta} \right)^4 \int_0^{\Theta'/T} \frac{x^3 dx}{e^x - 1} \right], \quad (14)$$

where $\Theta' k_B = E_1 - E_2$ is the energy difference between the two sites. This formula gave a good fit to the data with the following parameters:

$$\begin{aligned} \nu_0(0) &= 2006.3 \pm 2.0 \text{ MHz}, \\ \delta\nu_0 &= 31 \pm 3 \text{ MHz}, \\ \Theta' &= 55 \pm 14 \text{ K}, \\ C &= 0.68 \pm 0.05, \\ \Theta &= 655 \pm 25 \text{ K}, \end{aligned} \quad (15)$$

The solid line in Fig. 6 was calculated with these

values. The extrapolated hyperfine frequency $\nu_0(0)$ is compatible with the result obtained by the two-frequency method: $\nu_0(4.4\text{K})=2008\pm 2$ MHz, and the value of Θ is in reasonable agreement with the averaged Debye temperature of 625 K for Si quoted in the literature.²⁰

As seen in Eq. (12), the splitting $\delta\nu_0$ should cause an additional field-dependent relaxation λ_B of the triplet signals. However, within the proposed model it follows from the data of Bucci *et al.*¹⁷ that the hopping time τ_c at 4 K is approximately $0.1 \mu\text{s}^{-1}$. The expected effect $\lambda_B \simeq (\pi\delta\nu_{12})^2\tau_c$ is smaller than $0.3 \mu\text{s}^{-1}$ for fields up to 200 G. The observed damping of the direct transition at 18 K implies that τ_c is of the order of 1 ns at this temperature.

The values of $\delta\nu_0$ and Θ' should only be considered to be order-of-magnitude estimates since they depend on the assumption that there are only two sites with equal abundance. The data do not allow us to deduce more information in this respect.

We parenthetically remark that the zero-field signals of Mu^* were observed in the Si runs with a strong and temperature-independent relaxation of the order $10 \mu\text{s}^{-1}$ up to 150 K. A further increase of the temperature by 20 K caused the signals to disappear. No Mu^* signals were observed in the Ge runs.

C. Mu in Si, pressure dependence

The pressure dependence of the hyperfine frequency ν_0 of Mu in Si was measured at 273 K. The crystal was 20 mm in diameter and fitted snugly into the pressure cell described in Sec. II C. The cell was insulated by styrofoam and cooled by N_2 gas. The temperature was measured by three sensors attached to the cell at different places, continuously recorded and controlled within better than ± 0.1 K during the experiment. Four runs for each pressure point were performed with a change of the pressure between the individual runs. Small corrections were applied to the fitted ν_0 values, using $\partial\nu_0/\partial T$ ($T=273$ K) $= -0.55$ MHz/K from the data of Fig. 6, and then weighted averages were taken.

The results are shown in Fig. 9. No significant change of ν_0 with the pressure p is visible. A fit to a straight line gives

$$\frac{\partial\nu_0}{\partial p(T=273\text{ K})} = -0.12 \pm 0.13 \text{ MHz/kbar}, \quad (16)$$

$$\nu_0(T=273\text{ K}, p=0) = 1950.21 \pm 0.11 \text{ MHz}.$$

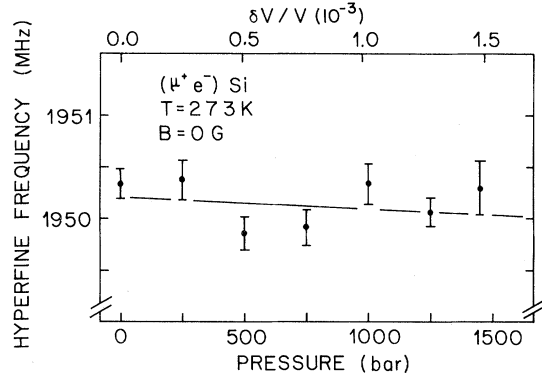


FIG. 9. Measured hyperfine frequencies ν_0 of Mu in Si at constant temperature $T=273$ K as a function of pressure or relative volume change.

Using the bulk modulus of Si ($B=980$ kbar),²⁸ the result may be expressed as a derivative with respect to the lattice constant a ,

$$\frac{1}{\nu_0} \frac{\partial\nu_0}{\partial a} = 0.078 \pm 0.084 \text{ \AA}^{-1}. \quad (17)$$

The change of a produced by the maximum pressure $P=1.5$ kbar is about 2 times larger than that by thermal lattice expansion between 120 and 300 K. This justifies the neglect of the latter in the analysis of the temperature-dependent data.

IV. DISCUSSION

For comparison, the experimental results to date on the temperature dependence of the hyperfine interaction HFI for Mu and Mu^* in the group-IV elements are collected in Table I. Two facts appear remarkable: (a) all coupling constants C are of order unity, and (b) the Θ agree well with the average Debye temperature $\bar{\Theta}_D$ from heat capacities. This agreement is particularly striking for Mu in Si and Mu^* in diamond,¹⁴ where the main variation of the HFI occurs at temperatures where $\bar{\Theta}_D$ is almost constant.²¹ Thus the phenomenological description of the effect in terms of the Debye model appears justified.

A variety of theoretical models have been proposed for Mu or the analogous hydrogen atom in Si and Ge. They may be divided into three classes:

(a) The effective-potential models²⁹ assume that the bound electron moves in a screened Coulomb potential. A space-dependent dielectric function $\epsilon(r)$ is used, which is unity near the muon (the origin), and which at large distances approaches ϵ_0 ,

TABLE I. Comparison of the experimentally determined constants of the temperature dependence of the HFI of Mu and Mu* according to the Debye model. The values for diamond are from Ref. 14, for Mu* in Si from Ref. 13, and for Mu* in Ge from Ref. 6. The averaged Debye temperature $\bar{\Theta}_D$ is from Ref. 20.

		Diamond	Silicon	Germanium
Mu	$\nu_0(0)$ (MHz)	3711(21)	2006(2)	2359.5(2)
	C		0.68(5)	0.27(7)
	Θ (K)		655(25)	273(26)
Mu*	$A_{\perp}(0)/h$ (MHz)	392.59(6)	92.59(5)	130.7(1.0)
	$A_{\parallel}(0)/h$ (MHz)	-167.98(6)	16.79(1)	26.8(1.0)
	C_{\perp}	0.38(2)	1.20(1)	
	C_{\parallel}	0.73(4)	0.52(11)	
	Θ (K)	1902(51)		
	$\bar{\Theta}_D$ (K)	1860	625	360

the static dielectric constant of the material. In the simplest case, usually referred to as the cavity model, one assumes that $\epsilon(r)=1$ inside a sphere of radius R , and $\epsilon(r)=\epsilon_0$ outside.

(b) In the chemical models^{30,31} based on the Hückel theory molecular orbitals are calculated for clusters of 30–40 atoms around a muon or proton.

(c) Pseudopotential methods^{32,33} explicitly take into account the band structure of the host. The charge density around the proton is calculated in a self-consistent way.

All models appear to give HFI's substantially reduced with respect to the vacuum value. At present however, the agreement between experimental and theoretical values of ν_0 from the more sophisticated models of type (b) and (c) is not better than from the models of type (a).

For a comparison with the experimental results of this paper only the models (a) are easily adaptable. With the cavity model, ν_0 can be calculated³⁴ as a function [$\nu_0(V)$] of the volume V of the cavity. The thermal lattice vibrations cause fluctuations δV of this volume and to lowest-order produce a shift of the measured ν_0 proportional to the second derivative of $\nu_0(V)$ and the thermal average $\langle \delta V^2 \rangle$. With the assumption of a Debye phonon spectrum, this gives a coupling constant $C=0.5 \times 10^{-3}$, i.e., the correct sign but an absolute value which is 3 orders of magnitude too small.

A prediction of the pressure dependence of ν_0 should be more reliable since the cavity radius is proportional to the lattice constant a . Depending where the radius for zero pressure is assumed, one gets $(1/\nu_0)(\partial\nu_0/\partial a)=0.15-0.32 \text{ \AA}^{-1}$, which is compatible with the experimental limits given by Eq. (17).

According to the calculations of Singh *et al.*³⁰

[type (b)], hydrogen (or muonium) should occupy the tetrahedral interstitial site in Si. Furthermore the published contour map shows a very deep energy minimum which would exclude diffusion at low temperatures, as is suggested by the experimental results.

In Sec. III B we postulated two sites for Mu in Si which according to Eq. (15) should be only slightly different. One may speculate that these sites are crystallographically equivalent and differ only because the neighboring Si atoms are different isotopes. Assuming the tetrahedral site, then it follows from the composition of natural Si (92.2 at. % ²⁸Si, 4.7 at. % ²⁹Si, and 3.1 at. % ³⁰Si) that in 30% of all cases one nearest neighbor (NN) is a heavy isotope and in the other 70% all NN are ²⁸Si. A different mass m of a NN causes a change in the vibrational amplitude and may also imply a shift of Mu from its normal equilibrium position. From Eq. (10) it follows that there is a sizable effect of the lattice zero-point motion on ν_0 of 170 MHz. Since the constant C is proportional to $m^{-3/2}$ (see Ref. 12 for the appropriate formulas), ν_0 would be reduced by about 20 MHz for a crystal of ³⁰Si, which is the right order of magnitude.

In Ge a monotonic $\nu_0(T)$ was observed in contrast to Si. It is notable that natural Ge consists of five different isotopes with similar abundances and is therefore very different from Si in this respect. The many different configurations possible probably do not result in a systematic effect.

There are also indications of Mu diffusion in Ge. The direct transition at 4.2 K showed a large relaxation rate $\lambda_0=10 \pm 4 \mu\text{s}^{-1}$, indicating a similar effect as in Si (Fig. 7). At the same temperature and with the same crystal the triplet signals¹⁹ gave $\lambda_t \simeq 0.3 \mu\text{s}^{-1}$, whereas at higher temperatures λ_t

was equal to λ_0 within statistical uncertainties of about $1-2 \mu\text{s}^{-1}$. The small value of λ_t at 4.2 K is also hard to explain if one considers the interaction of the ^{73}Ge nuclear dipoles with a stationary Mu. Experiments with a isotopically enriched Ge crystal are presently in preparation, and these should shed more light on the questions of isotope effects.

The amplitude a_0 of the direct transition was always found to be substantially smaller than theoretically expected from the amplitudes of the low-frequency triplet signal. This is mainly caused by the finite time resolution of the detectors [see Eq. (7)]. A reduction of a_0 could also result if there is a delay between a muon stop in the sample and the formation of Mu. If a short-lived, nonparamagnetic precursor state is transformed into Mu with a $\exp(-t/\tau)$ law, an additional reduction of a_0 by a factor $1/[1+(2\pi\nu_0\tau)^2]^{1/2}$ would result.³⁵

A comparison of the results obtained with different detectors, and measurements of the detector resolution with ^{60}Co sources and the muon beam, showed that no such effect is necessary to explain the reduction of a_0 and placed an upper limit on τ of 100 ps.

V. CONCLUSIONS

A new method for studying muonium in solids has been introduced. At comparatively low instrumental expense, it allows accurate measurements of the hyperfine frequency ν_0 which are superior to the traditional two-frequency method, in particular when there is spin relaxation.

The measured temperature dependence of ν_0

could be accurately accounted for with a Debye model. The possibility that lattice expansion plays a significant role was ruled out by an experiment with high pressure. It appears that the shift of the hyperfine interaction due to acoustic phonons is a common phenomena for the muonium states in diamond, Si and Ge and, moreover, that it has a similar magnitude in all cases.

The experiments showed that different transitions between Mu hyperfine levels may have very different relaxation rates. The observation of a large relaxation rate λ_0 for the direct transition and at the same time a small relaxation rate λ_t for the intra-triplet transitions for Mu in Si and in Ge at low temperature strongly suggests that Mu is very mobile in these materials.

Quantitative results for the diffusion constant should be obtained by accurately measuring λ_t at very low temperatures ($T < 4$ K). Ge appears preferable for this experiment since larger effects are expected than for Si.

ACKNOWLEDGMENTS

I wish to thank Professor W. Kündig, Dr. P. F. Meier, and Dr. B. D. Patterson for the help with the experiments, for many helpful discussions and for their critical reading of the manuscript. I am grateful to Dr. H. Graf and Dr. A. Weidinger (University Konstanz) for the loan of the Ge crystal. I am indebted to S. Estreicher for numerical results about the cavity model and to Dr. W. Reichart for his help with the on-line computing. This work was supported by the Swiss National Science Foundation.

¹G. Feher, R. Prepost, and A. M. Sachs, *Phys. Rev. Lett.* **5**, 515 (1960).

²B. Eisenstein, R. Prepost, and A. M. Sachs, *Phys. Rev.* **142**, 217 (1966).

³D. G. Andrianov, E. V. Minaichev, G. G. Myasishcheva, Y. V. Obukhov, V. S. Roganov, G. I. Savel'ev, V. G. Firsov, and V. I. Fistul, *Zh. Eksp. Teor. Fiz.* **58**, 1896 (1970) [*Sov. Phys.—JETP* **31**, 1019 (1970)].

⁴I. I. Gurevich, I. G. Ivanter, E. A. Meleshko, B. A. Nikol'skii, V. S. Roganov, V. I. Selivanov, V. P. Smiga, B. V. Sokolov, and V. D. Shestakov, *Zh. Eksp. Teor. Fiz.* **60**, 1896 (1970) [*Sov. Phys.—JETP* **33**, 253 (1971)].

⁵J. H. Brewer, K. M. Crowe, F. N. Gygax, R. F. Johnson, B. D. Patterson, D. G. Fleming, and A. Schenck, *Phys. Rev. Lett.* **31**, 143 (1973).

⁶E. Holzschuh, H. Graf, E. Recknagel, A. Weidinger,

Th. Wichert, and P. F. Meier, *Phys. Rev. B* **20**, 4391 (1979).

⁷D. E. Casperson, T. W. Crane, V. W. Hughes, P. A. Souder, R. D. Stambough, P. A. Thompson, H. Orth, G. zu Putlitz, H. F. Kaspar, H. W. Reist, and A. B. Denison, *Phys. Lett.* **59B**, 397 (1975).

⁸J. H. Brewer and K. M. Crowe, *Ann. Rev. Nucl. Part. Sci.* **28**, 239 (1978).

⁹E. Holzschuh, W. Kündig, and B. D. Patterson, *Helv. Phys. Acta* **54**, 552 (1981).

¹⁰C. Boekema, A. B. Denison, W. Kündig, W. Reichart, and K. Rüegg, *Helv. Phys. Acta* **52**, 376 (1979).

¹¹G. Balzer, H. Graf, E. Recknagel, A. Weidinger, and Th. Wichert, *Hyperfine Interact.* **2**, 603 (1981).

¹²E. Šimánek and R. Orbach, *Phys. Rev.* **145**, 191 (1966).

¹³K. W. Blazey, J. A. Brown, D. W. Cooke, S. A. Dodds,

- T. L. Estle, R. H. Heffner, M. Leon, and D. A. Vanderwater, *Phys. Rev. B* **23**, 5316 (1981).
- ¹⁴E. Holzschuh, W. Kündig, P. F. Meier, B. D. Patterson, J. P. F. Sellschop, M. C. Stemmet, and H. Appel, *Phys. Rev. A* **25**, 1272 (1982).
- ¹⁵B. D. Patterson, W. Kündig, P. F. Meier, F. Waldner, H. Graf, E. Recknagel, A. Weidinger, Th. Wichert, and A. Hintermann, *Phys. Rev. Lett.* **40**, 1347 (1978).
- ¹⁶C. Boekema, E. Holzschuh, W. Kündig, P. F. Meier, B. D. Patterson, W. Reichart, and K. Rüegg, *Hyperfine Interact.* **8**, 401 (1981).
- ¹⁷C. Bucci, R. De Renci, G. Guidi, P. Podini, R. Tedeschi, and L. O. Norlin, *Hyperfine Interact.* **8**, 385 (1981).
- ¹⁸C. W. Clawson, K. M. Crowe, S. S. Rosenblum, and J. H. Brewer, *Hyperfine Interact.* **8**, 397 (1981).
- ¹⁹A. Weidinger, G. Balzer, H. Graf, E. Recknagel, and Th. Wichert, *Phys. Rev. B* **24**, 6185 (1981).
- ²⁰J. de Launay, in *The Theory of Specific Heats and Lattice Vibrations*, Vol. 2 of *Solid States Physics*, edited by F. Seitz and D. Turnbull (Academic, New York, 1956).
- ²¹G. Dolling and R. A. Cowley, *Proc. Phys. Soc. London* **88**, 463 (1966).
- ²²R. Calvo and R. Orbach, *Phys. Rev.* **164**, 284 (1967).
- ²³W. T. Doyle and A. B. Wolbarst, *J. Phys. Chem. Solids* **36**, 549 (1975).
- ²⁴J. S. Shah and M. E. Straumanis, *Solid State Commun.* **10**, 159 (1972).
- ²⁵K. G. Lyon, G. L. Salinger, and C. A. Swenson, *J. Appl. Phys.* **48**, 865 (1977).
- ²⁶A. B. Denison, H. Graf, W. Kündig, and P. F. Meier, *Helv. Phys. Acta* **52**, 460 (1979).
- ²⁷I. G. Ivanter and V. P. Smilga, *Zh. Eksp. Teor. Fiz.* **54**, 559 (1968) [*Sov. Phys.—JETP* **27**, 301 (1968)].
- ²⁸*American Institute of Physics Handbook*, 3rd ed. (McGraw-Hill, New York, 1972).
- ²⁹J. S. Wang, and C. Kittel, *Phys. Rev. B* **7**, 713 (1973).
- ³⁰V. A. Singh, C. Weigel, J. W. Corbett, and L. M. Roth, *Phys. Status Solidi B* **81**, 637 (1977).
- ³¹A. Coker, T. Lee, and T. P. Das, *Hyperfine Interactions* **4**, 821 (1978).
- ³²W. E. Pickett, L. M. Cohen, and C. Kittel, *Phys. Rev. B* **20**, 5050 (1979).
- ³³C. O. Rodriguez, M. Jaros, and S. Brand, *Solid State Commun.* **31**, 43 (1979).
- ³⁴E. Holzschuh, S. Estreicher, W. Kündig, P. F. Meier, B. D. Patterson, J. P. F. Sellschop, M. C. Stemmet, and H. Appel, *Hyperfine Interact.* **9**, 611 (1981).
- ³⁵P. F. Meier, *Phys. Rev. A* **25**, 1287 (1982).